



In vivo metabolism study of rhubarb decoction in rat using high-performance liquid chromatography with UV photodiode-array and mass-spectrometric detection: A strategy for systematic analysis of metabolites from traditional Chinese medicines in biological samples

Rui Song^{a,b}, Lei Xu^b, Fengguo Xu^b, Zhe Li^b, Haijuan Dong^b, Yuan Tian^b, Zunjian Zhang^{a,b,*}

^a Department of Pharmaceutical Analysis, China Pharmaceutical University, Tongjia Lane 24, Nanjing 210009, China

^b Key Laboratory of Drug Quality Control and Pharmacovigilance (China Pharmaceutical University), Ministry of Education, Nanjing 210009, China

ARTICLE INFO

Article history:

Received 11 March 2010

Received in revised form 24 August 2010

Accepted 8 September 2010

Available online 17 September 2010

Keywords:

Rhubarb decoction

Metabolites

In vivo metabolism

HPLC–DAD

HPLC–MS/MS

ABSTRACT

High-performance liquid chromatography with diode-array detection (HPLC–DAD) and tandem mass spectrometry (HPLC–MS/MS) was used for separation and identification of metabolites in rat urine, bile and plasma after oral administration of rhubarb decoction. Based on the proposed strategy, 91 of the 113 potential metabolites were tentatively identified or characterized. Besides anthraquinones metabolites, gallic acid, (–)-epicatechin and (+)-catechin metabolites were also detected and characterized in these biological samples. Our results indicated that glucuronidation and sulfation were the main metabolic pathways of anthraquinones, while methylation, glucuronidation and sulfation were the main metabolic pathways of gallic acid, (–)-epicatechin and (+)-catechin. Phase I reactions (e.g., hydroxylation and reduction) played a relatively minor role compared to phase II reactions in metabolism of phenolic compounds of rhubarb decoction. The identification and structure elucidation of these metabolites provided essential data for further pharmacological and clinical studies of rhubarb and related preparations. Moreover, the results of the present investigations clearly indicated the relevance and usefulness of the combination of chromatographic, spectrophotometric, and mass-spectrometric analysis to detect and identify metabolites.

© 2010 Elsevier B.V. All rights reserved.

1. Introduction

Rhubarb (*Rhei Radix et Rhizoma*), one of the commonly used traditional Chinese medicines (TCMs), which is called Dahuang in Chinese, is derived from the dried roots and rhizomes of *Rheum officinale* Baill., *R. palmatum* L., or *R. tanguticum* Maxim. ex Balf. [1]. In general, its traditional usage is to be prepared as a decoction either alone or together with other crude drugs (such as *Aurantii Immaturus Fructus*, *Magnoliae Officinalis Cortex* and *Gardeniae Fructus*) for oral administration.

Pharmacological studies indicate that rhubarb has various bioactivities, such as purgative [2,3], antiviral [4,5], antibacterial [6], anti-inflammatory [7,8], protecting effects in rat with chronic renal failure [9,10], anti-angiogenic [11], antioxidative [12,13], inhibiting epoxidase [14], immunomodulatory [15], protecting vascular endothelium and alveolar epithelium [16].

Clinical researches show that rhubarb can significantly improve brachial artery endothelial function in patients with atherosclerosis [17], and ameliorate intestinal permeability in septic patients [18].

Regarding the chemical constituents of rhubarb, more than 100 compounds have been isolated and identified up to now, such as sennosides, anthraquinones, tannin and related compounds, phenylbutanones, naphthalins, stilbenes, polysaccharides and organic acid [19].

Although many investigations have been conducted in the fields of pharmacology, clinical trials, and phytochemistry about rhubarb, researchers still do not know what its effective constituents are, how many compounds are absorbed into blood after oral administration of the decoction, and what the fate of the decoction in the body is. The limited knowledge about the metabolism of rhubarb decoction restricts the deeper pharmacological mechanism study and wider clinical use of rhubarb.

In our previous study, chemical information of rhubarb decoction had been successfully analyzed using HPLC–DAD and HPLC–MS/MS, and 98 major constituents were tentatively identified. Data obtained from the fragmentation pathways analysis of the parent compounds greatly facilitated the identification of metabolites from rhubarb decoction, as most of these metabo-

* Corresponding author at: Center for Instrumental Analysis, China Pharmaceutical University, Tongjia Lane 24, Nanjing 210009, China. Tel.: +86 25 8327 1454; fax: +86 25 8327 1454.

E-mail address: zunjianzhangcpu@hotmail.com (Z. Zhang).

lites remained the structural features of the parent compounds. Thus, in the present study, our aim was to thoroughly profile the metabolism of rhubarb decoction using a three-step strategy, including rapid identification of the type of metabolites according to characteristic losses, metabolites identification, and determination of the most like conjugation site for phase II metabolites. This analytical strategy was proposed mainly based on the following hypothesis (1) *in vivo* metabolites transformed from a certain compound contain common chemical moieties from which the common fragment ions can be produced in tandem mass spectrometry, and (2) the structural difference between parent compound and its corresponding metabolite can be elucidated from the changes of UV absorption maxima in their UV spectra, especially for the 1,8-dihydroxyanthraquinone derivatives and their phase II metabolites.

Our results indicated, with the benefit of the UV information, the structure of many phase II metabolites of 1,8-dihydroxyanthraquinone derivatives in rhubarb decoction can be conclusively determined which could not be achieved by LC-MS/MS alone. Moreover, the results of the present investigations clearly indicated the relevance and usefulness of the combination of chromatographic, spectrophotometric, and mass-spectrometric analysis to detect and identify metabolites.

2. Experimental

2.1. Chemicals and materials

Gallic acid (GA, Molecular Weight (MW), 170), (+)-catechin (C, MW, 290), (–)-epicatechin (EC, MW, 290), emodin (MW, 270), chrysophanol (MW, 254), rhein (MW, 284), aloe-emodin (MW, 270) and physcion (MW, 284) were purchased from the Chinese National Institute for the Control of Pharmaceutical and Biological Products (Beijing, China). Methanol (HPLC grade) was purchased from VWR International Company (Darmstadt, Germany). Formic acid (analytical reagent) was purchased from the First Chemical Company of Nanjing (Jiangsu, China). Water was distilled twice before use. Rhubarb was purchased from Li County, Gansu Province, China, and authenticated by Prof. Ping Li (Key Laboratory of Modern Chinese Medicines, Ministry of Education, China Pharmaceutical University, Nanjing, China).

2.2. Preparation of rhubarb decoction

Fifteen grams of rhubarb were immersed in 150 mL-distilled water for 1 h and refluxed for 40 min at 100 °C, the aqueous extract was filtered, and the residue was refluxed for 20 min with another 150 mL-distilled water under the same conditions. The two water extracts were combined and condensed to 100 mL and stored at 4 °C until use.

2.3. Animals

Male Sprague–Dawley rats (body weight 200–250 g) were obtained from the Animal Multiplication Center of Qinglong Mountain (SCXK 2007-0007). They were kept in an environmentally controlled breeding room with standard laboratory food and water for one week prior to the experiments. All animals were fasted for 16 h with water *ad libitum* prior to the administration of rhubarb decoction.

Six male rats were first administered an oral dose of 10 mL/kg of normal saline and held in metabolic cages for the collection of 1.5 h blank urine samples. Then these rats were exposed orally to the rhubarb decoction at a dose of 10 mL/kg. Urine samples collected during 0–1.5 h were discarded and then these rats were administered an oral dose of 10 mL/kg rhubarb decoction again. Finally,

urine samples collected during 0–3 h after the second administration were adopted as drug-containing samples. Male rats were fixed on a wooden plate and anesthetized with ether. An abdominal incision was made and the common bile duct was cannulated using polyethylene tubing for collection of the bile samples, and closed by suture. Each rat was administered oral doses of 10 mL/kg rhubarb decoction by oral gavage when the rat recovered to consciousness, and the bile samples were collected for 3 h. Heparinized blank blood samples of 500 µL were collected from four rats from the ophthalmic veins of the rats by sterile capillary tube, then, each rat was administered oral doses of 10 mL/kg rhubarb decoction every 30 min, after the third administration, blood samples were collected at 0.5 h from the ophthalmic veins of the rats. Blood samples were shaken up and centrifuged at 2950 × g for 10 min. The supernatants were decanted. All biological samples were stored at –70 °C until addition extraction and analysis. The experiments were carried out in accordance with the Guidelines for Animal Experimentation of China Pharmaceutical University (Nanjing, China) and the protocols were approved by the Animal Ethics Committee of this institution.

2.4. Extraction of rat biological samples

An aliquot of 10 mL urine samples was added 30 mL methanol to precipitate protein, and then centrifuged at 2950 × g for 10 min. The supernatant was concentrated to ca. 1 mL under reduced pressure, and then mixed with 1 mL methanol. After centrifuged at 13,800 × g for 10 min, 10 µL aliquots of supernatant were used for analysis.

The bile samples and plasma samples were added 2 volumes of methanol to precipitate proteins, and then centrifuged at 2950 × g for 10 min. The supernatant from drug-containing plasma samples was concentrated to ca. 2 mL under reduced pressure. All of the supernatant was further centrifuged at 13,800 × g for 10 min, 10 µL aliquots of supernatant were used for analysis.

2.5. HPLC–DAD analysis

The analyses were performed using an Agilent Series 1100 liquid chromatograph (Agilent Technologies, Palo Alto, CA, USA), equipped with a diode-array detector that recorded UV spectra in the range of 190–400 nm. Chromatography was carried out on an Agilent Zorbax SB-C₁₈ column (250 mm × 4.6 mm, 5 µm). The mobile phase consisted of 0.1% formic acid (A) and methanol (B), using a gradient elution of 5% B at 0–10 min, 5–20% B at 10–30 min, 20–25% B at 30–40 min, 25–45% B at 40–160 min, 45–60% B at 160–180 min, 60–80% B at 180–200 min, and 80% at 200–220 min. The flow rate was 1 mL/min. The detection wavelengths were set at 280 nm. The column oven temperature was set at 30 °C throughout the whole analytical procedure. Data were acquired and processed by HP ChemStation software.

2.6. HPLC–MS/MS analysis

The LC condition for the metabolites of rhubarb decoction was the same as described above except that the effluent was directed to source at the rate of 0.3 mL/min via a T-union splitting. HPLC–MS/MS analysis was performed with a Finnigan TSQ Quantum Discovery MAX system (triple quadrupole mass spectrometer, applied by Thermo Electron, San Jose, CA, USA) connected to a Finnigan Surveyor HPLC system (Thermo Electron, San Jose, CA, USA) via an ESI interface. Data were acquired and processed by Xcalibur 2.0 controlling software. The spray voltage was set at –3800 V. The capillary voltage was fixed at –15 V, and the temperature was maintained at 350 °C. The tube lens offset voltage was set at –30 V. The HPLC fluid was nebulized using N₂, which was also the sheath gas and the auxiliary gas set at 40 arbitrary units and 10 arbitrary

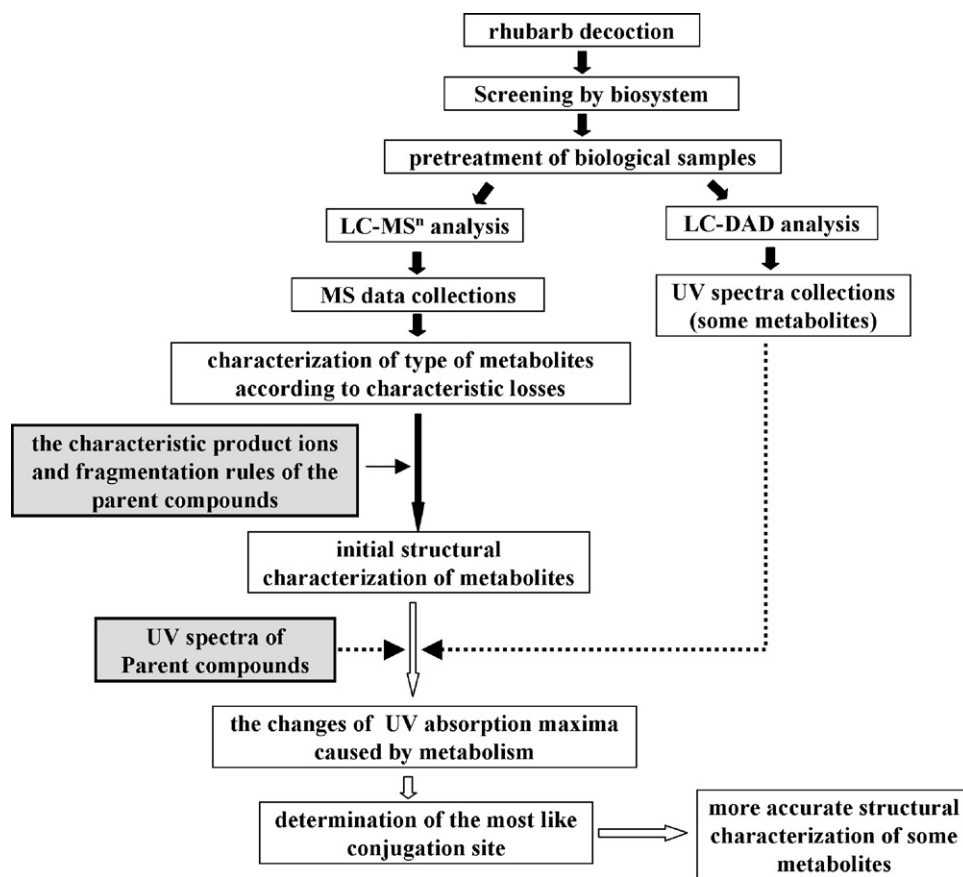


Fig. 1. Summary diagram of presently developed approach for identification of metabolites from rhubarb decoction in biological samples.

units, respectively. Argon was used as collision gas at a pressure of 1.5 mTorr. The collision energy for collision-induced dissociation (CID) was initially set at 30 V for all of the preferred ions and then modified according to the fragments.

The metabolites analysis of rhubarb decoction in rat biological samples by HPLC–MS/MS was achieved by two steps, which is: (1) full mass range scan analysis of the blank and drug-containing samples, from m/z 120 to 1000, centroid mode. The m/z values of the possible metabolites were obtained according to the differences of the two total ion current (TIC) chromatograms. Furthermore, the LC retention times of the possible metabolites were also obtained. (2) The mass scan time segment was divided into several parts according to acquired retention time information of potential targets obtained from step (1) (the possible metabolites). Each time segment included several scan events that were set to acquire a targeted product scan of the pre-setting m/z values of the assumed metabolites.

2.7. Strategy for systematic analysis of metabolites from rhubarb decoction in biological samples

The first step of this strategy was to characterize the type of metabolites formed through the different metabolic routes according to characteristic losses detectable in MS/MS experiments. Collision-induced dissociation, as studied by tandem mass spectrometry, allowed the rapid identification of the type of conjugate. Diagnostic losses corresponding to conjugates have been summarized in the published literature [20], such as $C_6H_8O_6$ (176 Da) for glucuronide conjugates and SO_3 (80 Da) for sulfate conjugates.

The second step was to identify metabolites on the basis of full understanding of the characteristic product ions and fragmentation

rules of the parent compounds (reference standard). The identification of the metabolites and elucidation of their structure were performed by comparing the changes in molecular masses (ΔM) and MS/MS spectral patterns of metabolites with those of parent compounds.

The third step was to determine exact conjugation site for some metabolites in order to give more accurate structural characterization. This kind of further identification was mainly referred to the metabolites of 1,8-dihydroxyanthraquinone derivatives. The alteration of absorption maximum could be used to determine the exact conjugate site of phase II metabolites of 1,8-dihydroxyanthraquinone derivatives. For example, all phenolic phase II metabolites of rhein show a hypsochromic shift of 19–24 nm, whereas conjugation at the carboxyl group does not alter the absorption maximum, and the bisether/ether-glucuronidation results in a stronger hypsochromic shift of 60 nm leading to a λ_{max} value of 370 nm [21]. However, this step was unnecessary for metabolites that existed at an extremely trace level or overlapped with other compounds because of the absence of UV spectra. The general procedures of our strategy and approach were summarized into a diagram as shown in Fig. 1.

3. Results and discussion

3.1. Optimization of HPLC and MS conditions

To obtain HPLC chromatograms with good separation and peak shape, different mobile phase compositions were screened. Given the acidity of phenolic compounds, it was found that methanol and 0.1% aqueous formic acid were the most suitable eluting solvent system. The separation efficiency was somewhat affected by tem-

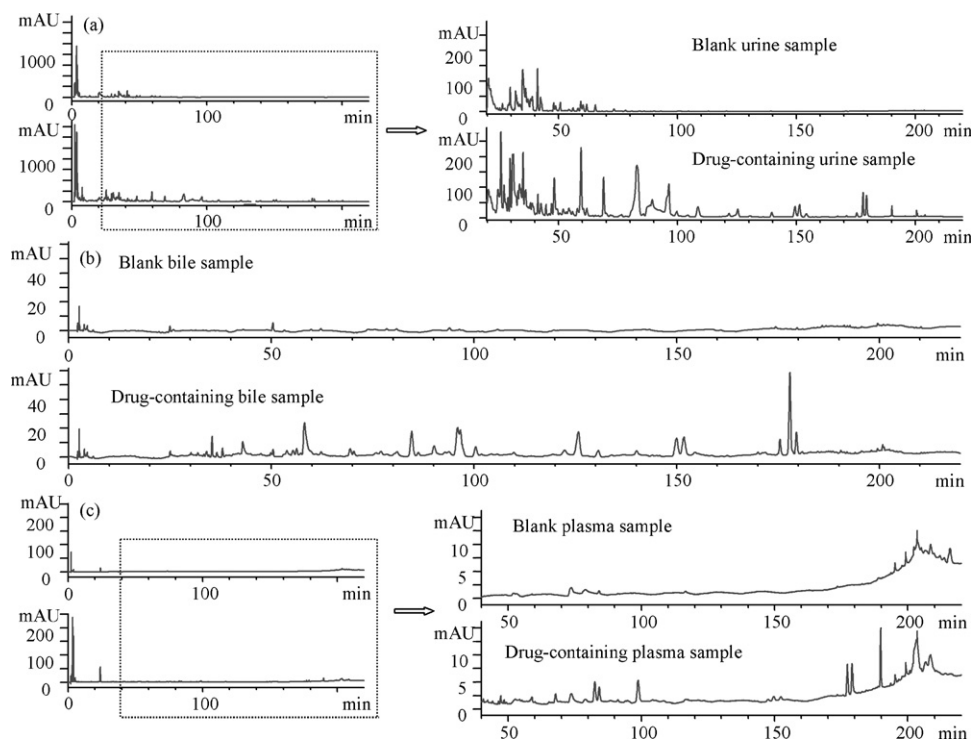


Fig. 2. HPLC–DAD chromatograms monitored at 280 nm of rat (a) urine, (b) bile, and (c) plasma before and after administration of rhubarb decoction.

perature, and better separation was achieved at 30 °C. The proposed method was acceptable as well as adequate for further MS/MS analysis. To acquire maximum sensitivity for most compounds, MS parameters such as spray voltage, capillary temperature, sheath gas and auxiliary gas pressure, source CID, collision gas pressure and collision energy were optimized using acetonitrile extraction of rhubarb decoction by flow injection analysis (FIA). It was found that the negative ion mode was more sensitive than positive ion mode for most of the compounds with triple quadrupole mass spectrometer, so negative ion mode was chosen.

3.2. Fragmentation behavior and UV absorbance of the parent compounds

To interpret the mass spectra of the metabolites using the LC/MS technique, it is necessary to fully understand the fragmentation behavior of the parent compound. According to our previous studies on the chemical information of rhubarb decoction, galloylglucoses, flavan-3-ols and anthraquinones are three main constituents. Therefore, GA, C(EC) and five free anthraquinones (emodin, chrysophanol, rhein, aloë-emodin and physcion) were selected as representative parent compounds in this study. The UV spectra, chemical structures and MS/MS spectra of $[M-H]^-$ ion of GA, C and EC were shown in Fig. S-1. The UV spectra, chemical structures and ESI–MS/MS fragmentation behaviors of five free anthraquinones were reported in our previous publication [22]. As most of these metabolites remained the structural features of the parent compounds, the analysis of the fragmentation pathways greatly facilitated the identification of metabolites from rhubarb decoction.

3.3. Peak detection in biological samples by HPLC–DAD and HPLC–MS/MS

Fig. 2 shows the HPLC–DAD chromatograms monitored at 280 nm of blank and corresponding drug-containing biological

samples. As for MS detection, the potential metabolites were detected from drug-containing biological samples by comparison of the TIC chromatograms of the drug-containing samples with those of blank samples. The retention time of each potential metabolite was ascertained by employing its mass to generate its extracted ion chromatogram (EIC) of the drug-containing sample (Fig. 3). Compared with blank samples, a total of 113 metabolites were detected in extracted ion chromatograms from the drug-containing urine, bile and plasma (Table 1). The available UV spectra of metabolites were partly presented in Fig. S-2.

3.4. Identification of metabolites

The identification of metabolites was carried out according to the approach shown in Fig. 1. Metabolite M59 was selected as an example for the stepwise elucidation of the molecular structure. The structural elucidations of the other metabolites were carried out similarly.

M59 gave a $[M-H]^-$ molecule at m/z 621. A CID product ion spectrum of M59 with collision energy of 30 V displayed fragment ion at m/z 445, 269, 175 and 85 (Fig. 4(a)). It was found that both the $[M-H-176]^-$ and $[M-H-2 \times 176]^-$ ions, plus the ion at m/z 175 were observed. So, M59 was identified as the metabolite that conjugated with two molecules of glucuronic acid. The aglycone ion at m/z 269 could produce fragment ions at m/z 252, 240 and 223 under CID conditions with collision energy of 45 V (Fig. 4(b)). According to our previous studies on ESI–MS/MS fragmentation behaviors of aloë-emodin [22], the aglycone of M59 was assigned as aloë-emodin. However, as shown in Fig. 4(c), there are three hydroxyl groups available in the structure of aloë-emodin. MS/MS data can unambiguously prove the glucuronidation of a hydroxyl group, but usually do not allow to differentiate among the three possible glucuronidation sites, as the MS/MS spectra of the isomers differing only in their substitution pattern are almost undistinguishable. But in this case, the extract conjugate site could be determined by comparing the UV spectrum of M59 with that of parent compound

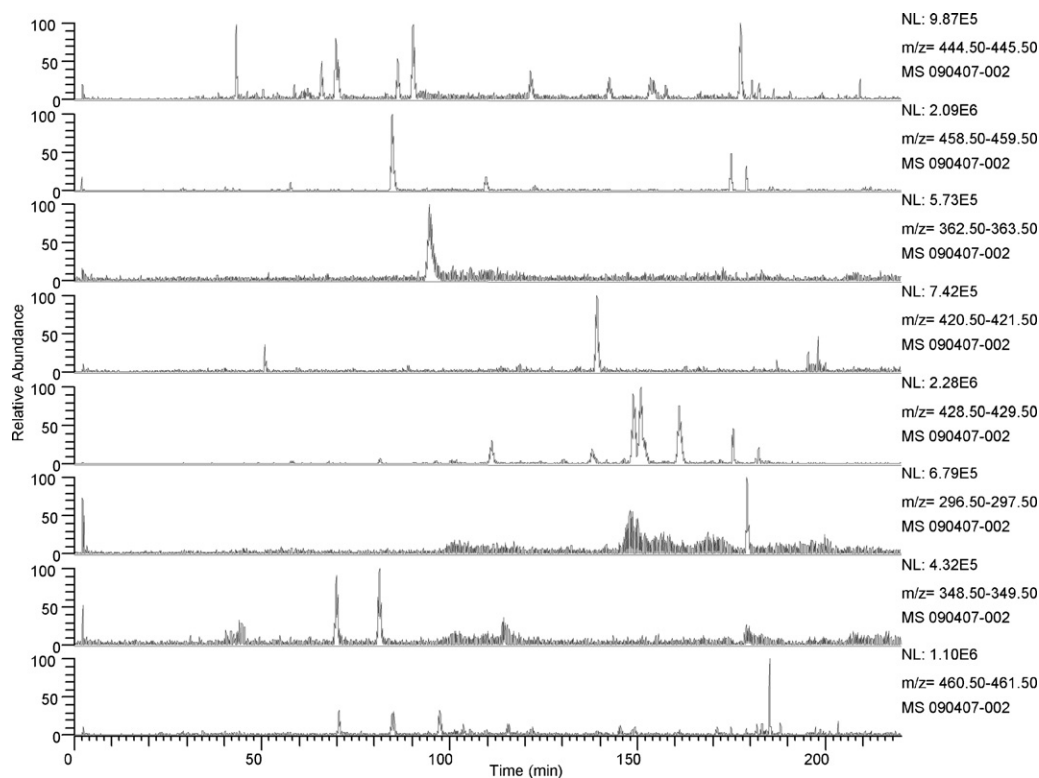


Fig. 3. The extracted ion chromatograms of the $[M-H]^-$ ions of some metabolites detected from drug-containing bile.

(aloe-emodin). The bisglucuronidation resulted in a strong hypsochromic shift leading to a λ_{\max} value of 380 nm (Fig. 4(d)), which suggested that M59 was aloe-emodin-1,8-diglucuronides.

The identification of the other metabolites and elucidation of their structures were performed mainly based on their MS/MS fragmentations. In addition, the difference between UV spectrum

of interest and that of parent compound was also considered in the structural elucidation only if the UV spectrum of the interest was available. Ultimately, 91 of the 113 potential metabolites were tentatively identified, and could be generally divided into three groups: gallic acid-related, flavan-3-ols-related and anthraquinones-related metabolites.

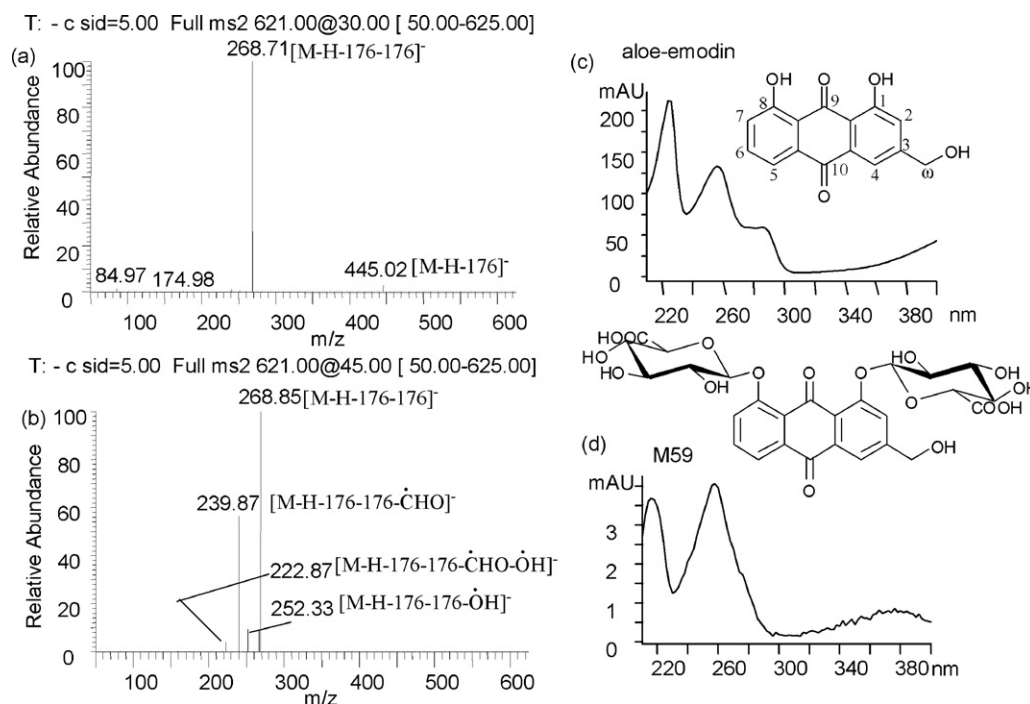


Fig. 4. MS/MS spectra of M59 with the collision energy of (a) 15 V and (b) 45 V; UV spectra and chemical structures of (c) aloe-emodin and (d) M59.

Table 1
The metabolites detected in rat urine (U), bile (B) and plasma (P) after oral administration of rhubarb decoction.

No.	t _R (min)	[M–H] [–]	U	B	P	No.	t _R (min)	[M–H] [–]	U	B	P	No.	t _R (min)	[M–H] [–]	U	B	P	No.	t _R (min)	[M–H] [–]	U	B	P
M1	3.71	301	+	–	–	M24	25.65	369	+	–	–	M47	39.80	449	+	–	–	M70	58.12	473	+	–	–
M2	6.25	521	+	–	–	M25 ^a	26.01	465	+	–	–	M48	40.35	407	+	–	–	M71 ^a	59.17	598	–	+	–
M3	6.60	331	+	–	–	M26	26.02	690	+	–	–	M49 ^a	42.20	479	+	–	–	M72	60.37	409	–	+	–
M4	7.20	345	+	–	–	M27	26.53	559	+	–	–	M50	43.70	479	+	–	–	M73 ^a	60.75	525	–	+	–
M5	8.11	331	+	–	–	M28	26.55	369	+	–	–	M51	43.28	465	+	–	–	M74	61.34	313	–	+	–
M6	9.03	169	+	–	–	M29	27.05	690	+	–	–	M52	46.11	383	+	–	–	M75 ^a	70.04	349	–	+	–
M7	9.20	345	+	–	–	M30 ^a	27.14	465	+	–	–	M53	46.31	409	+	–	–	M76 ^a	70.65	461	–	+	–
M8	9.45	331	+	–	–	M31	27.18	559	+	–	–	M54	49.00	365	+	–	–	M77 ^a	71.30	445	–	+	–
M9	11.31	331	+	–	–	M32	29.38	369	+	–	–	M55	49.93	621	+	–	–	M78	77.14	447	–	+	–
M10	11.50	521	+	–	–	M33	29.80	369	+	–	–	M56	50.49	387	–	+	–	M79	81.11	593	–	+	–
M11	15.35	521	+	–	–	M34	30.40	449	+	–	–	M57	50.51	311	+	–	–	M80	83.22	349	–	+	–
M12	15.92	521	+	–	–	M35 ^a	30.31	559	+	–	–	M58 ^a	50.73	607	+	–	–	M81	83.36	459	–	+	–
M13	16.15	359	+	–	–	M36	30.92	559	+	–	–	M59 ^a	51.20	621	+	–	–	M82	85.88	459	–	+	–
M14	17.32	345	+	–	–	M37	33.45	465	+	–	–	M60	53.80	387	–	+	–	M83 ^a	86.25	445	–	+	–
M15	18.38	263	+	–	–	M38	34.36	465	+	–	–	M61	54.73	621	–	+	–	M84 ^a	90.5	363	–	+	–
M16	18.90	359	+	–	–	M39 ^a	35.20	373	–	+	–	M62	55.04	355	–	+	–	M85	91.30	407	–	+	–
M17	19.80	345	+	–	–	M40	35.34	465	+	–	–	M63	55.04	568	–	+	–	M86 ^a	92.50	445	–	+	–
M18	20.43	263	+	–	–	M41	35.15	559	+	–	–	M64	55.95	607	–	+	–	M87	93.82	371	–	+	–
M19	20.65	359	+	–	–	M42	35.53	559	+	–	–	M65	56.52	403	–	+	–	M88 ^a	95.40	363	–	+	–
M20	21.01	465	+	–	–	M43 ^a	35.85	479	+	–	–	M66	56.55	415	–	+	–	M89 ^a	97.80	591	–	+	–
M21	21.65	263	+	–	–	M44	38.52	383	+	–	–	M67	56.74	621	–	+	–	M90 ^a	98.75	591	–	+	–
M22	22.98	465	+	–	–	M45 ^a	39.30	383	+	–	–	M68	56.82	607	–	+	–	M91 ^a	101.74	605	–	+	–
M23	23.50	263	+	–	–	M46 ^a	39.46	277	–	+	–	M69 ^a	57.60	459	–	+	–	M92	104.53	621	–	+	–

^a UV spectrum of the metabolite is available.

3.4.1. Identification of gallic acid-related metabolites

A total of 23 compounds detected in rat urine, bile and plasma were tentatively assigned as metabolites originating from GA and galloylglucoses (Table S-1). Except M46, all of the GA-related metabolites were identified only on the basis of their mass spectra. Besides GA (M6) and four galloylglucoses (M3, M5, M8 and M9), 13 glucuronide conjugates (M1, M2, M4, M7, M10–M14, M16, M17, M19 and M39) and 5 sulfate conjugates (M15, M18, M21, M23 and M26) were characterized as GA-related metabolites. They could be further classified into three subgroups according to their MS data (Table S-1). Metabolites in subgroup 1, including M1–M9, M14 and M17, yielded characteristic ions at *m/z* 169 and 125. Among them, M1 showed a deprotonated molecule [M–H][–] at *m/z* 301. Its MS/MS fragmentation was predominated by the elimination of glucuronidyl residue to give ion at *m/z* 125. According to the MS data and metabolic fate of gallic acid in rat [23,24], M1 was identified as pyrogallol-O-glucuronide. Metabolites in subgroup 2 (M10–M13, M15, M16, M18, M19, M21 and M23) had a series of product ions at *m/z* 183, 168 and 124, which suggested that the aglycone of these metabolites was methyl-O-gallic acid. As to metabolites in subgroup 3 (M39 and M46), the presence of characteristic ions at *m/z* 197, 182, 167 indicated that the aglycone should be dimethylated gallic acid.

3.4.2. Identification of flavan-3-ols-related metabolites

A total of 28 compounds were assigned as flavan-3-ols-related metabolites, including metabolites of (–)-epicatechin and (+)-catechin. Their mass data are summarized in Table S-2, and available UV spectra of metabolites are presented in Fig. S-2. Eight glucuronide conjugates (M20, M22, M25, M30, M37, M38, M40 and M51), six sulfate conjugates (M24, M28, M32, M33, M34 and M47) and the other two metabolites (M26 and M29) were assigned as (–)-epicatechin and (+)-catechin metabolites owing to the presence of some diagnostic ions related to (–)-epicatechin and (+)-catechin (Table S-2). Among them, M25 and M30 were further confirmed as (–)-epicatechin-O-glucuronide on the basis of similarity of their UV spectra with that of (–)-epicatechin. M26 and M29 all gave an [M–H][–] molecule at *m/z* 690, and yielded a series of characteristic ions at *m/z* 465, 369, 289 and 245. Based on these evidences, M26 and M29 were tentatively assigned as positional isomers of (–)-epicatechin-5-S-acetylcysteine-7-O-glucuronide-3'-O-sulfate or (+)-catechin-5-S-acetylcysteine-7-O-glucuronide-3'-O-sulfate.

Six compounds (M27, M31, M35, M36, M41 and M42) conjugated with glucuronic acid and sulfuric acid, three glucuronide conjugates (M43, M49 and M50) and three sulfate conjugates (M44, M45 and M52) were assigned as metabolites that possessed the aglycone of methylated EC or C due to the presence of the aglycone ion at *m/z* 303, 14Da (CH₂) higher than the *m/z* values of the deprotonated molecular ions of EC and C. Among them, according to the similarity of UV spectra with that of EC (Fig. S-2) and metabolic fate of EC in rat [25], M35 and M45 were further identified as 3'-O-methyl-(–)-epicatechin-O-glucuronide-O-sulfate and 3'-O-methyl-(–)-epicatechin-O-sulfate, while M43 and M49 were tentatively identified as positional isomers of 3'-O-methyl-(–)-epicatechin-O-glucuronide.

3.4.3. Identification of anthraquinones-related metabolites

Anthraquinones are the main bioactive constituents of rhubarb decoction. In this study, a total of 40 compounds detected in rat urine, bile and plasma were tentatively assigned as metabolites originating from anthraquinones. Among them, M69 was the phase II metabolite, and M76, M78 and M95 were the metabolites transformed from conjugation of phase II metabolites by glucuronidation. According to the aglycone of these metabolites (except M69), they were generally divided into six groups, named

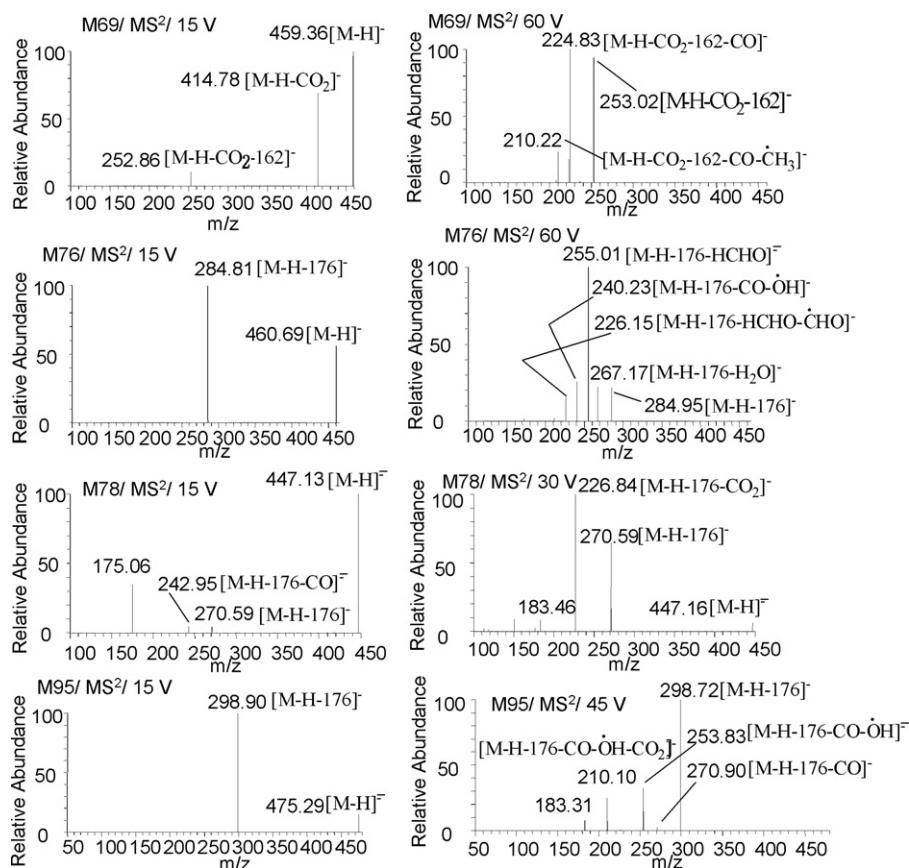


Fig. 5. MS/MS spectra of M69, M76, M78 and M95 under the CID conditions with different collision energy.

as G-A1 containing aloe-emodin (A1), G-A2 containing rhein (A2), G-A3 containing emodin (A3), G-A4 containing chryphanol (A4), G-A5 containing physcion (A5) and G-A6 containing laccac acid D (A6) as the aglycone.

Identification of metabolites in G-A1: Six glucuronide conjugates (M55, M58, M59, M76, M77 and M86) and two sulfate conjugates (M75 and M80) were assigned as metabolites of aloe-emodin. Among them, M55, M59, M75, M77, M80 and M86 comprised the same aglycone aloe-emodin (A1), and yielded characteristic ions of A1 at m/z 269 and 240. According to the MS data of M58, the presence of the characteristic ions of A1 indicated that the fragment ion at m/z 429 corresponded to aloe-emodin-O-glucoside. Moreover, the UV spectrum of M58 was similar with that of M59 (Fig. S-3). So, M58 was identified as aloe-emodin-8-O-glucoside-1-O-glucuronide or aloe-emodin-1-O-glucoside-8-O-glucuronide. As for M76, the aglycone ion $[M-H-C_6H_8O_6]^-$ at m/z 285 was 16 Da higher than the deprotonated ion of A1 (Fig. 5), suggesting that it was monohydroxylated aloe-emodin-O-glucuronide. Under the CID conditions with collision energy of 60 V, the MS/MS spectrum of M76 displayed ions of m/z 285, 267, 255, 240 and 226 (Fig. 5). According to our previous work concentrated on the *in vitro* metabolism of anthraquinone derivatives [22], the aglycone of M76 was assigned as 2-hydroxyaloe-emodin. Besides, by comparing the UV spectrum (Fig. S-2) of M76 with that of 2-hydroxyaloe-emodin [22], it was found that glucuronidation did not alter the absorption maximum, which suggested that M76 should be 2-hydroxyaloe-emodin- ω -O-glucuronide.

Identification of metabolites in G-A2: As listed in Table S-3, besides rhein (M107) and rhein-1-O-glucoside (M83), three glucuronide conjugates (M81, M82 and M93) and two sulfate conjugates (M84 and M88) were assigned as metabolites of rhein (A2). Because UV spectra of most of metabolites were available (Fig. S-2), further

identification of them was established based on their retention time and the similarity of their UV spectra with that of rhein.

Identification of metabolites in G-A3: A total of 13 compounds were assigned as metabolites of emodin. Their mass data are summarized in Table 2, and UV spectra of some metabolites are presented in Fig. S-4. Our results indicated that glucuronidation was the major metabolic pathway of emodin. Except M69, M78 and M95, all of the metabolites comprised the same aglycone emodin (A3), and yielded characteristic ions of A3 at m/z 269 and 225. M69 showed a deprotonated ion at m/z 459. Under the CID conditions with collision energy of 15 V, the MS/MS spectrum of M69 displayed fragment ions of m/z 415 and 253 (Fig. 5). The ion at m/z 415 was formed by the loss of CO₂ (-44 Da from the m/z value of the deprotonated molecule). The ion at m/z 253 was the further fragment of m/z 415 with the loss of anhydroglucose. In addition, further fragment ions at m/z 225 (loss of CO from m/z 253), and a less intense ion at m/z 210 (loss of methyl radical from m/z 225) appeared after heightening the collision energy to 60 V (Fig. 5). According to the information obtained from the MS/MS spectra of M69, it should be a metabolite generated by the oxidation of the hydroxyl group at C-3 position of emodin-O-glucoside. M78 and M95 were the glucuronides of phase I metabolites of emodin, which detected from the drug-containing bile. The aglycone of M78 was identified as 1,3,8-trihydroxy-6-methyl-10-oxanthranol, because the aglycone ion at m/z 271 and its product ions at m/z 243 and 227 (Fig. 5) were all 2 Da more than m/z 269 ($[M-H]^-$ ion of emodin) and its product ions at m/z 241 and 225. The elucidation could also be demonstrated by our previous study [26]. As for M95, the aglycone ion $[M-H-C_6H_8O_6]^-$ at m/z 299 was 30 Da higher than the deprotonated ion of emodin (Fig. 5). A CID product ion spectrum of m/z 475 (the deprotonated ion of M95) displayed three major fragment ions at m/z

Table 2 Mass data for identification of emodin-related metabolites in rat after oral administration of rhubarb decoction.

No.	t_R (min)	$[M-H]^-$	MS/MS	Urine	Bile	Plasma	Identification
M61	54.73	621	MS ² -30V [621]: 445(2), 283(7), 269(100) MS ² -45V [621]: 269(100), 241(16), 225(4), 205(15), 197(1)	+	-	-	Emodin-O-digluconides
M64	55.95	607	MS ² -15V [607]: 607(22), 445(64), 431(100), 269(16) MS ² -45V [607]: 269(100), 241(61), 225(3)	-	+	-	Emodin-O-glucoside-O-gluconide
M67	56.74	621	MS ² -30V [621]: 445(1), 283(4), 269(100), 225(5) MS ² -45V [621]: 269(100), 241(8), 225(11)	+	+	-	Emodin-O-digluconides
M68	56.82	607	MS ² -15V [607]: 607(100), 431(51), 268(93) MS ² -45V [607]: 268(100), 225(12)	-	+	-	Emodin-O-glucoside-O-gluconide
M69 ^a	57.60	459	MS ² -15V [459]: 459(100), 415(69), 253(11) MS ² -60V [459]: 253(94), 225(100), 210(23)	-	+	-	1,8-Dihydroxy-3-carboxy-6-methylanthraquinone-1or 8-O-gluconide
M73 ^a	60.75	525	MS ² -15V [525]: 525(100), 445(58), 269(99) MS ² -60V [525]: 269(34), 241(40), 225(100), 210(24), 197(10), 180(8)	-	+	-	Emodin-1 or 8-O-gluconide-3-O-sulfate or Emodin-1 or 8-O-sulfate-3-O-gluconide
M78	77.14	447	MS ² -15V [447]: 447(100), 271(5), 243(5), 175(35) MS ² -30V [447]: 447(8), 271(65), 227(100)	-	+	-	1,3,8-Trihydroxy-6-methyl-10-oxanthranol gluconide
M92	107.05	621	MS ² -15V [621]: 621(22), 445(100), 269(23) MS ² -60V [621]: 269(100), 241(35), 225(56), 197(2)	+	+	-	Emodin-O-digluconides
M94 ^a	124.40	445	MS ² -30V [445]: 269(100), 241(13), 225(24) MS ² -15V [475]: 475(15), 299(100)	+	+	-	1,3,8-Trihydroxy-6-(glucuronidyl)methylanthraquinone
M95	124.51	475	MS ² -45V [475]: 299(100), 271(3), 254(32), 211(8), 210(25), 183(8) MS ² -15V [445]: 445(34), 329(8), 269(100)	-	+	-	Emodic acid-O-gluconide
M102 ^a	157.15	445	MS ² -30V [445]: 292(2), 269(100), 241(3), 225(18), 210(5) MS ² -15V [445]: 445(6), 269(100)	+	+	+	Emodin-2-C-gluconide
M104 ^a	179.42	445		+	-	+	Emodin-3-O-gluconide

^a UV spectrum of the metabolite is available.

271, 254 and 210 (Fig. 5) According to our previous work concentrated on the *in vitro* metabolism of emodin [26], the aglycone of M95 was unambiguously assigned as emodic acid. M94, M102 and M104 all gave an $[M-H]^-$ molecule at m/z 445, and their MS/MS fragmentations were predominated by the elimination of glucuronidyl residue to give aglycone ions at m/z 269 as base peak. However, the UV spectra (Fig. S-4) and retention time (Table 2) of these three metabolites were quite different from each other. By comparing the UV spectra of them with that of emodin, the differences were attributed to glucuronidation of the exocyclic methyl group of emodin (M94), C-2-glucuronidation of emodin (M102), and glucuronidation of the C-2-hydroxy group of emodin (M104), respectively.

Identification of metabolites in G-A4: Five glucuronide conjugates (M89, M90, M91, M100 and M101) and one sulfate conjugates (M98) were assigned as metabolites of chrysophanol (A4). Their mass data are summarized in Table S-3, and UV spectra of some metabolites are shown in Fig. S-2. Among them, the UV spectra of M89–M91 are similar with that of M59 (Fig. S-3). In addition, the retention time of chrysophanol-1-O-glucoside is shorter than that of chrysophanol-8-O-glucoside in the reversed-phase chromatography system [27]. Therefore, M89, M90 and M91 were tentatively identified as chrysophanol-1-O-glucoside-8-O-gluconide, chrysophanol-8-O-glucoside-1-O-gluconide, and chrysophanol-1,8-biglucuronides, respectively. M100 and M101, which were simultaneously detected in rat urine, bile and plasma, were identified as chrysophanol-1-O-gluconide and chrysophanol-8-O-gluconide, respectively.

Identification of metabolites in G-A5: In the present study, altogether 4 glucuronide conjugates (M96, M97, M103 and M105) detected in rat urine and bile were assigned as metabolites of physcion (A5). The UV spectra of M96 and M97 (Fig. S-3) are similar with that of M59 but different from that of physcion. Based on the changes between them and A5 in UV absorbance and molecular masses (ΔM), M96 was identified as physcion-1-O-glucoside-8-O-gluconide or physcion-8-O-glucoside-1-O-gluconide, and M97 was identified as physcion-1,8-O-digluconides.

Identification of metabolites in G-A6: Besides unchanged laccic acid D (M106) detected in rat urine and plasma, one glucuronide conjugate (M70) detected in rat urine was assigned as metabolite of A6. Considering that 6-glucuronidation was relatively easier under the considerations of electronic effect and steric hindrance, M70 was tentatively identified as laccic acid D-6-O-gluconide.

3.5. Analysis of metabolite profile of rhubarb decoction

The metabolites tentatively identified in the present study provided a global view of rat metabolites after oral administration of rhubarb decoction. Gallic acid, flavan-3-ols and anthraquinones were observed in rat biological samples as the parent compounds or related metabolites, indicating that they could be absorbed into blood and accordingly might be responsible for curative effects of rhubarb decoction. Anthraquinones were undoubtedly the most prevalent metabolites in rat biological samples, especially in the drug-containing bile and plasma. Among the identified metabolites, 21 gallic acid-related metabolites, 23 flavan-3-ols-related metabolites and 31 anthraquinones-related metabolites were detected in the drug-containing urine, while the numbers were 2, 10, 27 and 1, 0, 7 in the drug-containing bile and plasma. Rat feces were also used to investigate the metabolism of rhubarb decoction. However, the feces of rats administered rhubarb decoction orally contained a few of compounds, such as unchanged (+)-catechin and rhein.

The detection of 4 galloylglucosides (M3, M5, M8 and M9), methyl-O-galloylglucose-O-gluconides (M10–M12) and anthraquinone-

O-glucoside-O-glucuronides (M58, M64, M68, M83, M89, M90 and M96) demonstrated that galloylglucoses and anthraquinone glucosides could be absorbed into the circulating system with no need to be hydrolyzed into the corresponding aglycones. According to the metabolites identified in rat bile, methylation reaction was the most common phase II reaction for gallic acid, (–)-epicatechin and (+)-catechin in rat liver, which was consistent with previous reports [23–25]. Furthermore, some metabolism information on phase I reactions of anthraquinones in rhubarb decoction such as hydroxylation, hydrogenation and oxidation could be obtained from these identified metabolites (M69, M76, M78 and M95). This was consistent with our previous study that concentrated on the *in vitro* metabolism of anthraquinones from rhubarb [22]. According to the present study, most of the metabolites of components of rhubarb decoction were formed through phase II metabolic route. Taking the metabolites originating from aloe-emodin for example, only M76 was the glucuronide of phase I metabolite of emodin, and its peak intensity (Fig. S-5) indicated that M76 was not the dominant metabolite of aloe-emodin. Therefore, we speculated that phase I reactions (e.g., hydroxylation and reduction) played a relatively minor role compared to phase II reactions (e.g., methylation, glucuronidation and sulfation) in metabolism of phenolic compounds of rhubarb decoction.

4. Conclusion

High-performance liquid chromatography with diode-array detection (HPLC–DAD) and tandem mass spectrometry (HPLC–MS/MS) was used for separation and identification of metabolites in rat urine, bile and plasma after oral administration of rhubarb decoction. Based on the provided strategy, 91 of the 113 potential metabolites detected in rat urine, bile and plasma were tentatively identified or characterized. Owing to the absence of UV spectra of some metabolites, their structures could not be definitely elucidated by LC–MS/MS. However, the present study still demonstrated the analytical potential of this approach for identification of metabolites. This identification and structure elucidation of these metabolites provided essential data for further pharmacological and clinical studies of rhubarb and related preparation.

Acknowledgements

This project was financially supported by Specialized Research Fund for TCM of State Administration of Traditional Chinese Medicine (no. 06-07ZP17), Chinese Natural Science Fund (no.

30672587) and Technology Innovation Program for post-graduate of Jiangsu province (no. CX08B_194Z).

Appendix A. Supplementary data

Supplementary data associated with this article can be found, in the online version, at doi:10.1016/j.chroma.2010.09.028.

References

- [1] The Pharmacopoeia Commission of People's Republic of China, Pharmacopoeia of the People's Republic of China, 2005 ed., Chemical Industry Press, Beijing, 2005, p. 17.
- [2] P.G. Xiao, L.Y. He, L.W. Wang, J. Ethnopharmacol. 10 (1984) 275.
- [3] Z. Zheng, C. Zhu, S. Gui, C. Lin, Zhong Yao Cai 25 (2002) 569.
- [4] D.O. Andersen, N.D. Weber, S.G. Wood, B.G. Hughes, B.K. Murray, J.A. North, Antivir. Res. 16 (1991) 185.
- [5] D.L. Barnard, J.H. Huffman, J.L.B. Morris, S.G. Wood, B.G. Hughes, R.W. Sidwell, Antivir. Res. 17 (1992) 63.
- [6] C. Jong-Chol, M. Tsukasa, A. Kazuo, K. Hiroaki, Y. Haruki, O. Yasuo, J. Ethnopharmacol. 19 (1987) 279.
- [7] Y. Liu, F. Yan, Y. Liu, C. Zhang, H. Yu, Y. Zhang, Y. Zhao, Phytother. Res. 22 (2008) 935.
- [8] M.K. Moon, D.G. Kang, J.K. Lee, J.S. Kim, H.S. Lee, Life Sci. 78 (2006) 1550.
- [9] T. Yokozawa, N. Suzuki, H. Oura, G. Nonaka, I. Nishioka, Chem. Pharm. Bull. 34 (1986) 4718.
- [10] J. Wang, Y. Zhao, X. Xiao, H. Li, H. Zhao, P. Zhang, C. Jin, J. Ethnopharmacol. 124 (2009) 18.
- [11] Z.H. He, M.F. He, S.C. Ma, P.P. But, J. Ethnopharmacol. 121 (2009) 313.
- [12] H. Matsuda, T. Morikawa, I. Toguchida, J.Y. Park, S. Harima, M. Yoshikawa, Bioorg. Med. Chem. 9 (2001) 41.
- [13] A. Iizuka, O.T. Iijima, K. Kondo, H. Itakura, F. Yoshie, H. Miyamoto, M. Kubo, M. Higuchi, H. Takeda, T. Matsumiya, J. Ethnopharmacol. 91 (2004) 89.
- [14] I. Abe, T. Seki, H. Noguchi, Y. Kashiwada, Planta Med. 66 (2000) 753.
- [15] L. Ma, Zhong Xi Yi Jie He Za Zhi 11 (1991) 418.
- [16] C. Li, J. Zhou, P. Gui, X. He, J. Tradit. Chin. Med. 21 (2001) 54.
- [17] X.L. Fang, Q. Fang, J.J. Luo, X. Zheng, Am. J. Chin. Med. 35 (2007) 929.
- [18] Y.F. Liu, H.M. Yu, C. Zhang, F.F. Yan, Y. Liu, Y. Zhang, M. Zhang, Y.X. Zhao, Am. J. Chin. Med. 35 (2007) 583.
- [19] D.H. Jiao, S.J. Du, The Study of Rhubarb, Shanghai Science & Technology Press, Shanghai, 2000, p. 291.
- [20] K. Levsen, H.M. Schiebel, B. Behnke, R. Dötzer, W. Dreher, M. Elend, H. Thiele, J. Chromatogr. A 1067 (2005) 55.
- [21] M. Dahms, R. Lotz, W. Lang, U. Renner, E. Bayer, H. Spahn-Langguth, Drug Metab. Dispos. 25 (1997) 442.
- [22] R. Song, H. Lin, Z.J. Zhang, Z. Li, L. Xu, H.J. Dong, Y. Tian, Rapid Commun. Mass Spectrom. 23 (2009) 537.
- [23] A.N. Booth, M.S. Masri, D.J. Robbins, O.H. Emerson, F.T. Jones, F. De Eds, J. Biol. Chem. 234 (1959) 3014.
- [24] L. Zong, M. Inoue, M. Nose, K. Kojima, N. Sakaguchi, K. Isuzugawa, T. Takeda, Y. Ogihara, Biol. Pharm. Bull. 22 (1999) 326.
- [25] M. Natsume, N. Osakabe, M. Oyama, M. Sasaki, S. Baba, Y. Nakamura, T. Osawa, J. Terao, Free Radic. Biol. Med. 34 (2003) 840.
- [26] R. Song, F.G. Xu, Z.J. Zhang, Y. Liu, H.J. Dong, Y. Tian, Biomed. Chromatogr. 22 (2008) 1230.
- [27] M. Ye, J. Han, H.B. Chen, J.H. Zheng, D.A. Guo, J. Am. Soc. Mass Spectrom. 18 (2007) 82.